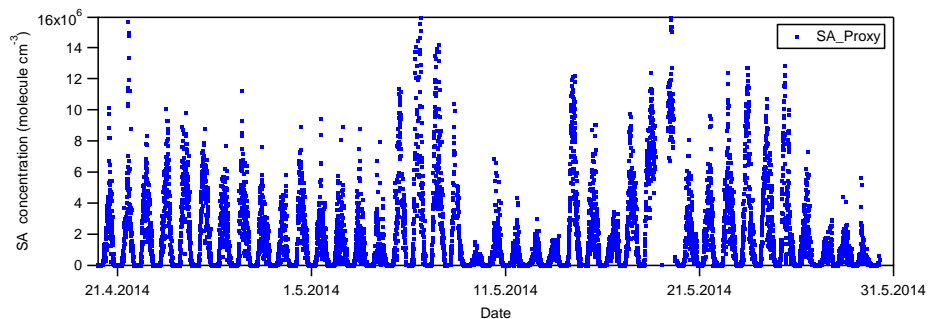Atmospheric
Chemistry
and Physics

Supplement of

Combined effects of boundary layer dynamics and atmospheric chemistry on aerosol composition during new particle formation periods
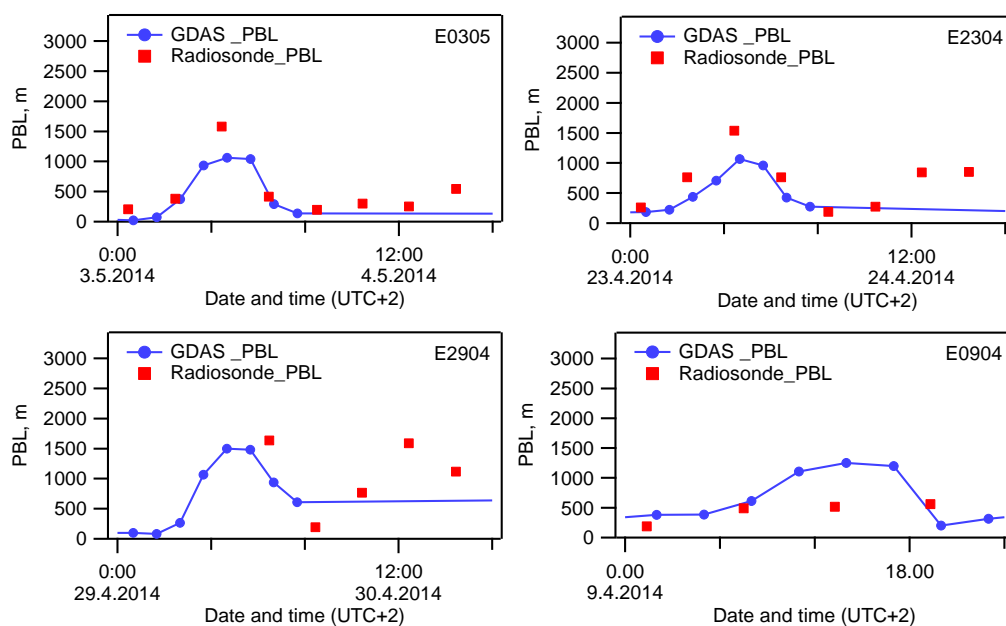
Liqing Hao et al.

Correspondence to: Liqing Hao (hao.liqing@uef.fi) and Annele Virtanen (annele.virtanen@uef.fi)

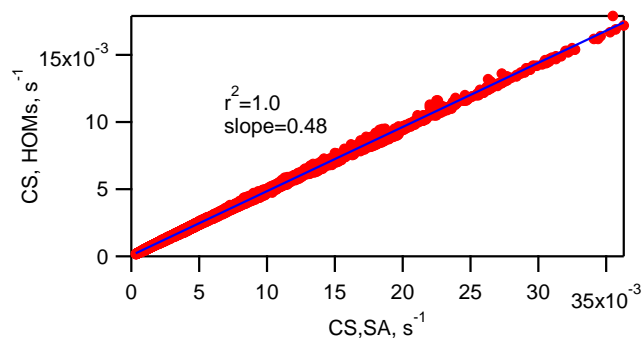**Figure S1.** Sulfuric acid concentrations approximated by proxy approach in the campaign.

Figure S2. The height of planetary boundary layer (PBL) from GDAS modelling (in blue) and radiosonde (in red) in the nucleation events in this study.

Figure S3. Comparison of condensation sink for sulfuric acid (SA) and HOMs in the campaign.
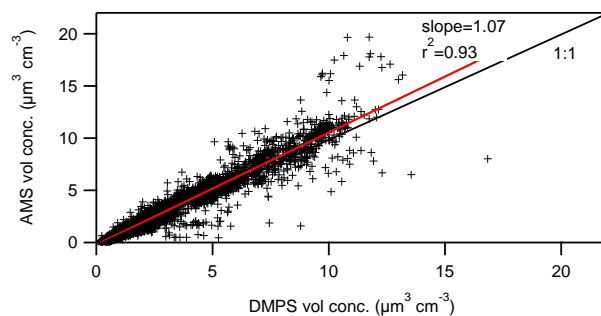
Figure S4. Comparison the volume concentrations of measurements between AMS and DMPS in this study.

Figure S5. The chosen new particle formation event as an example.

Sec. S1. Diagnostics evaluation of PMF results

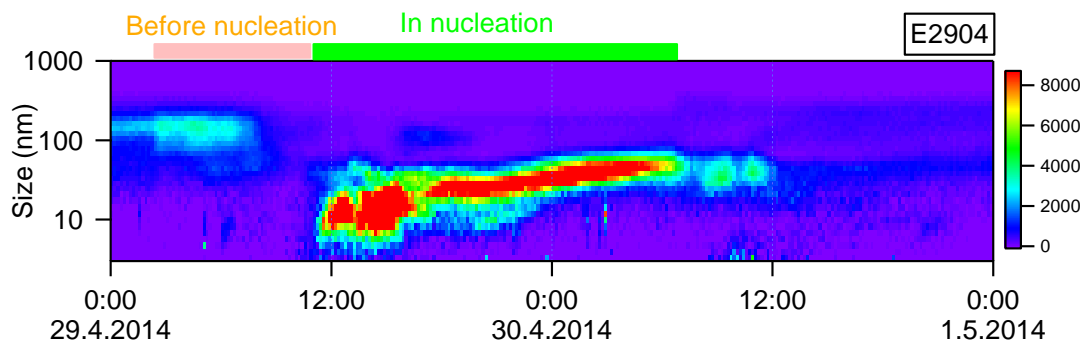The key PMF diagnostic plots are shown in Fig. S6. A 5-factor solution was chosen and Fpeak=0 was selected (Fig S7). A 4-factor solution did not extract out an inorganic factor and thus misses one meaning factor compared to a 5-factor solution (Fig. S8). A 6-factor solution split SVOOA2 of 5-factor solution to two sub-SVOOA factors and did not produce more meaningful factors (Fig. S9).
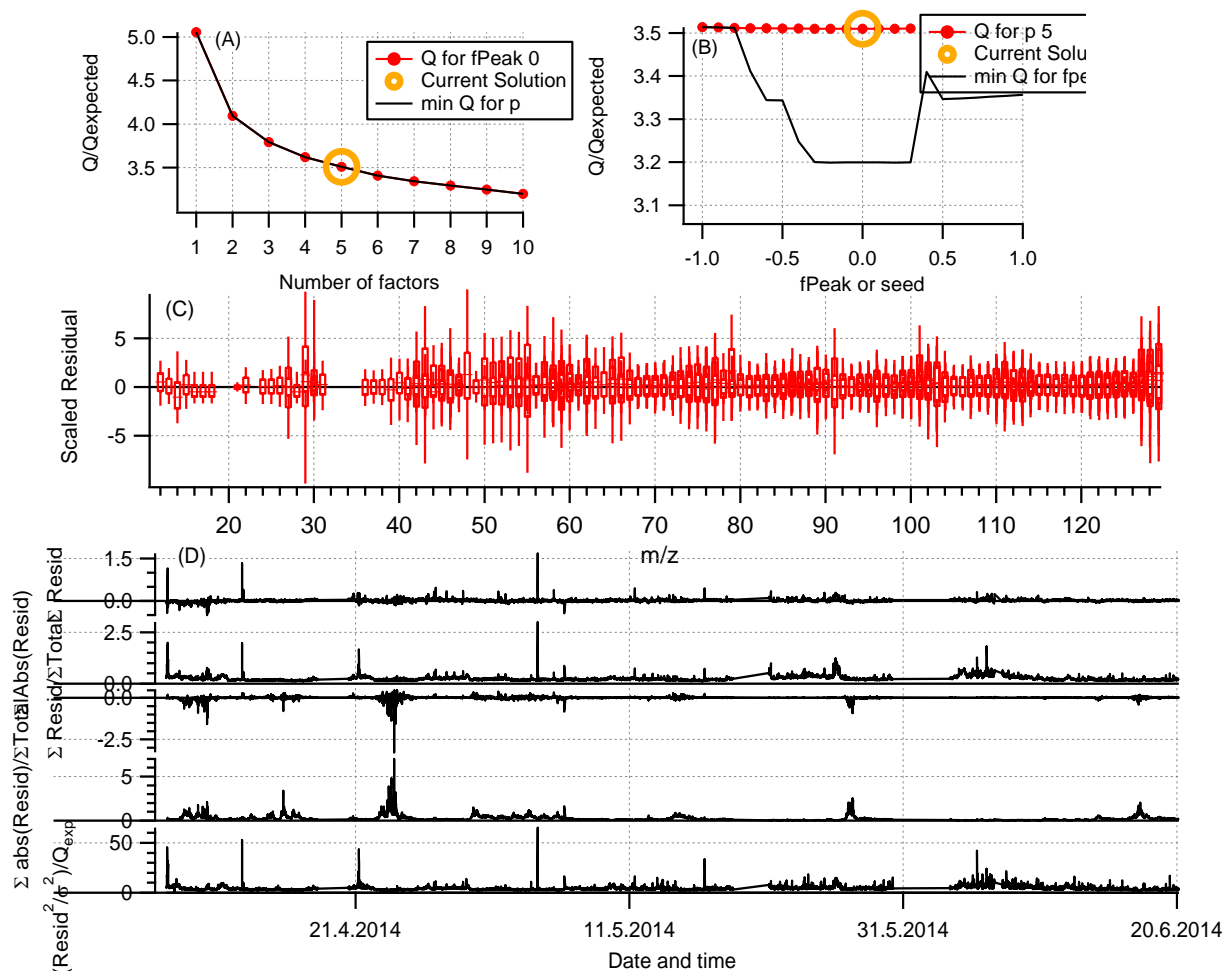
Figure S6. PMF key diagnostics plots: (a) $Q/Q_{expected}$ varies as function of PMF factor at fPeak 0; (b) $Q/Q_{expected}$ varies as function of rotational ambiguity; (c) Scaled residual for each mass; (d) time series of the total residual and Q/Q expected contribution for every point during this study. For more details on PMF and the interpretation of these plots see Ulbrich et al. (2009).
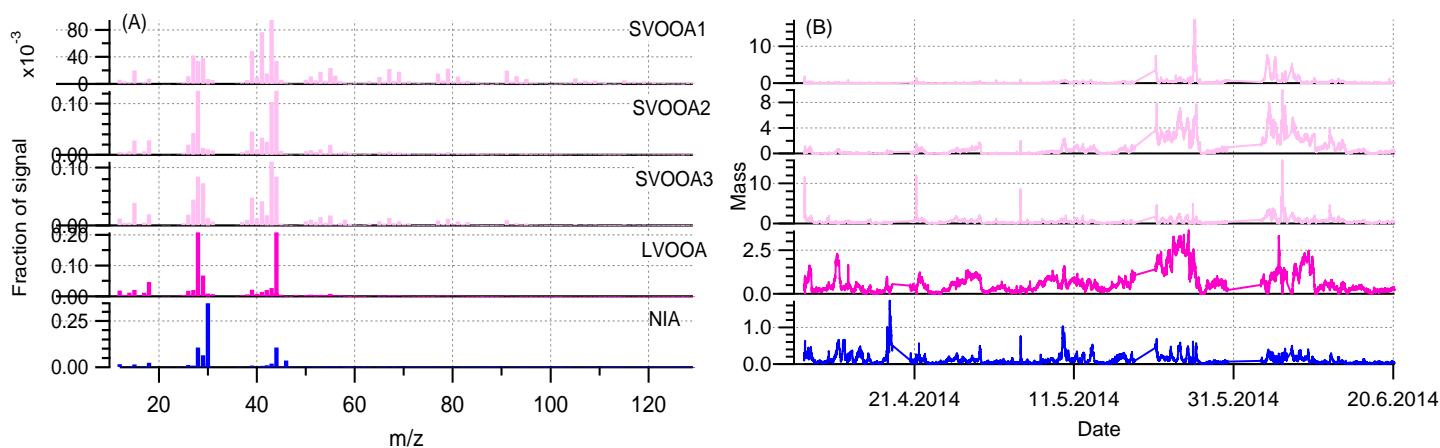
Figure S7. Time series (a) and mass profiles (b) by PMF analysis at 5-factor solution.
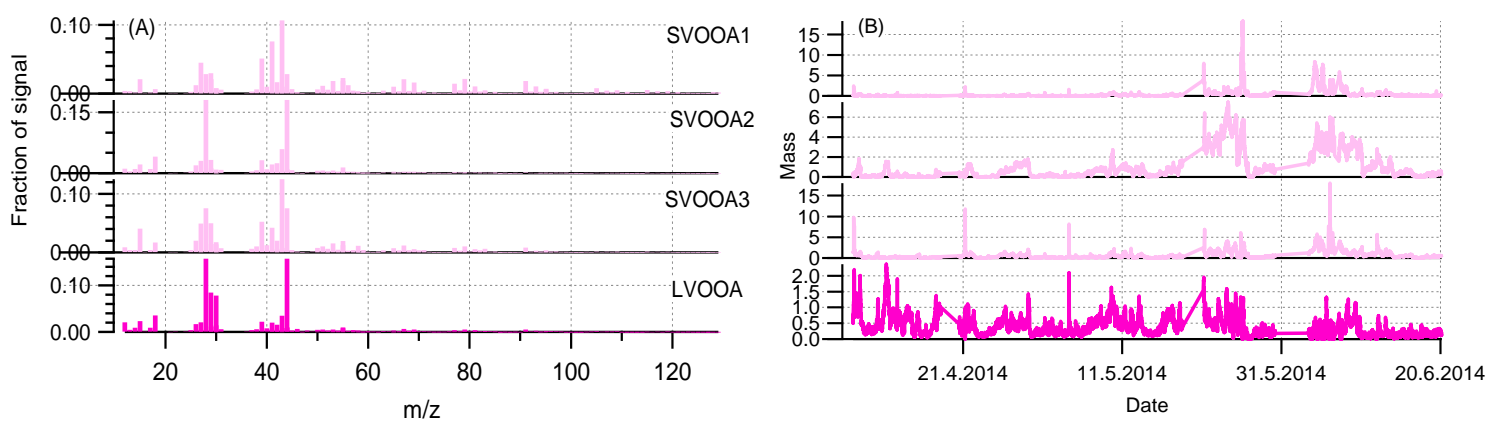
Figure S8. Time series (a) and mass profiles (b) by PMF analysis at 4-factor solution.
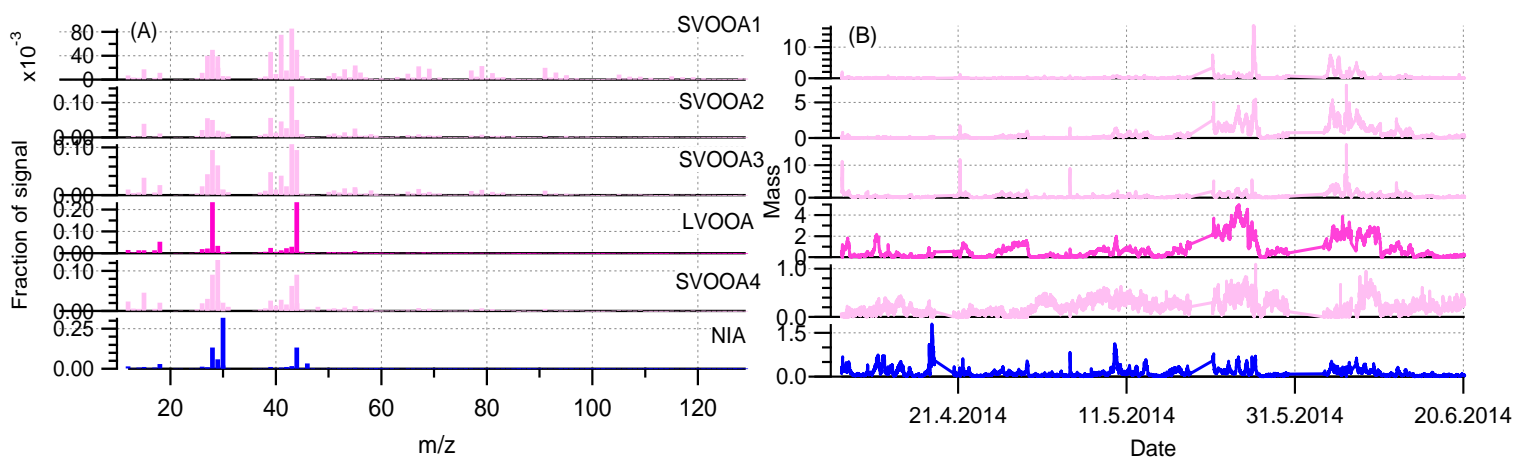
Figure S9. Time series (a) and mass profiles (b) by PMF analysis at 6-factor solution

Sec. S2. Operation of PTR-MS

The gas VOCs were monitored by a proton transfer reaction time-of-flight mass spectrometer (PTR-ToF-MS) (Ionicon Analytik GmbH, Jordan et al., 2009). The PTR-MS was measuring from six levels of a 73m-high mast. The ground level data (4.2 m above the ground) was used in this study. Calibration of the instrument was performed with the calibration gas containing 16 compounds in a mass range from 33 to 180 amu. Detailed measurement procedure and data analysis refer to Rantala et al. (2014) and Schallhart et al. (2016).

Sec. S3. Aerosol components by PMF

To gain insight into detailed relative variation of individual components, a PMF analysis of the high-resolution organic mass spectra together with NO^+ and NO_2^+ ions was conducted. In this study, a 5-factor solution at Fpeak=0 was chosen. The mass spectra profiles and time series of the five factors are shown in Fig. S10. The organic component in this study was resolved into one LVOOA (low volatility oxygenated organic aerosol) factor and three SVOOA (semi-volatile OOA) factors. The factors SVOOA1, SVOOA2 and SVOOA3 were merged to generate a new factor by means of a mass-weighted combination, representing a combined less oxygenated organic factor. As a result, an improved three-factor solution is reported in this paper (refer to Fig. S11).
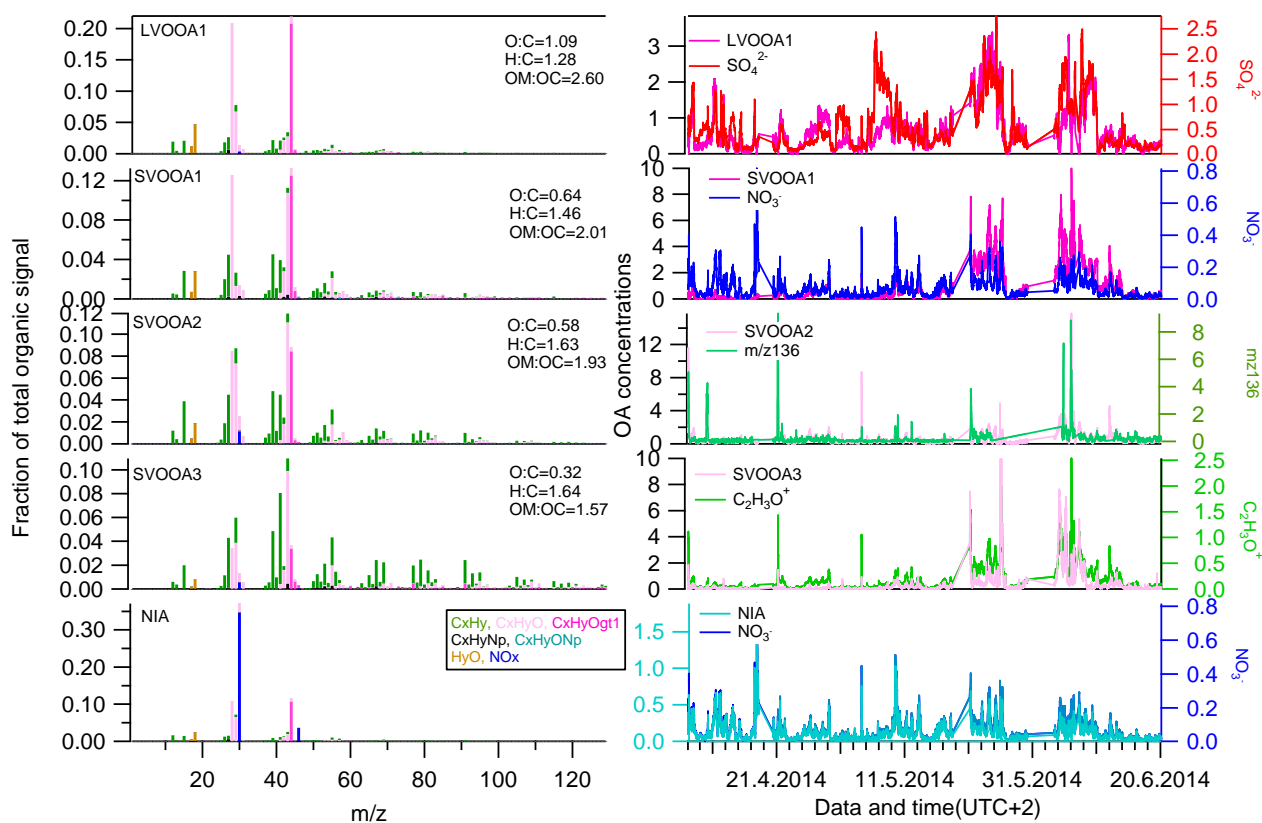

Figure S10. PMF factor solutions to the high-resolution mass spectra during the entire campaign: profiles and time series and the corrections with the tracers. All species except for monoterpene are in unit of μg m^{-3}.
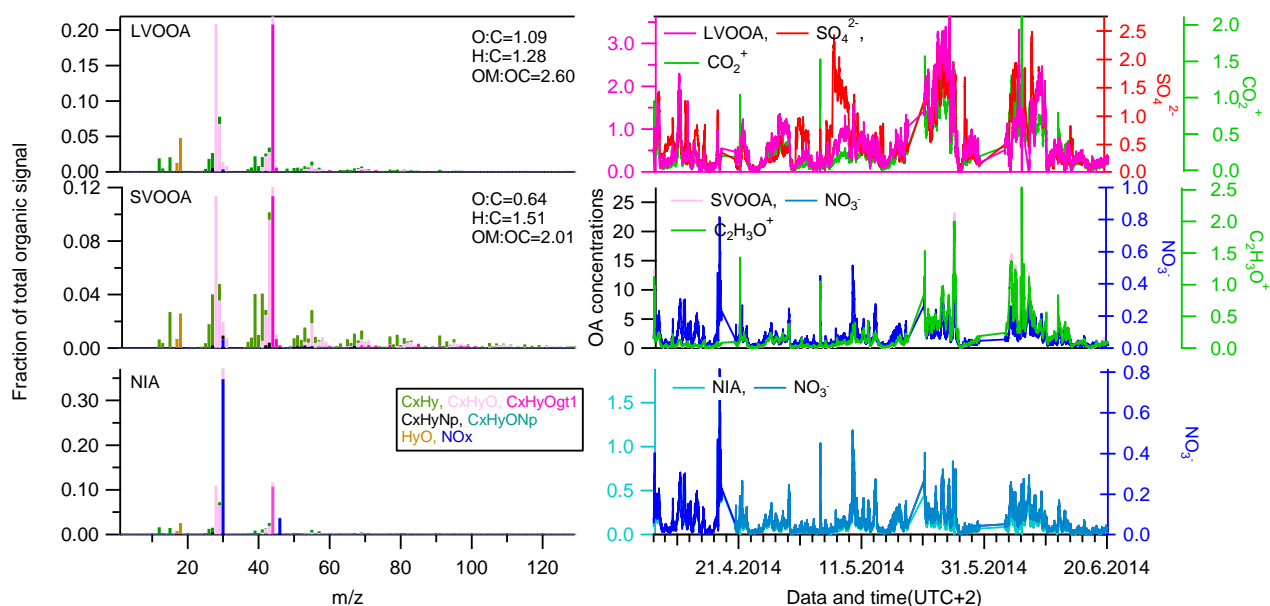
Figure S11. The improved PMF 3-factor solutions to the high-resolution mass spectra during the entire campaign: profiles and time series and the corrections with the tracers. All species except for monoterpene are in unit of μg m⁻³.

The mass spectrum of LVOOA is dominated by the peaks at m/z 44 (mostly CO_2^+) and m/z 28 (CO^+) with a high O/C ratio of 1.09. The mass spectrum pattern resembles OOA-1 and LVOOA determined by PMF in the same measurement site (Raatikainen et al., 2010; Corrigan et al., 2013; Kortelainen et al., 2016) and also the LVOOA at a global scale (Ng et al., 2010). The time series of LVOOA moderately correlates with sulfate species (r^2=0.54, Fig. S12A), indicating a source of regional transport. The mass spectrum of the other OOA component, SVOOA, has prominent fragment at m/z 43 (dominated by $C_2H_3O^+$). It is similar to the previously reported biogenic OOA component in the same site (Corrigan et al., 2013) and the biogenic secondary organic aerosol (SOA) from laboratory chamber studies (e.g. Kiendler-Scharr et al., 2009; Hao et al., 2009). Its O/C ratio is 0.64 and the time series shows excellent correlations with m/z43 ions (r^2=0.99, Fig. S12B). SVOOA is also in line with the variations of monoterpene concentrations measured by PTR-MS, implying the nature of a local source of SVOOA.
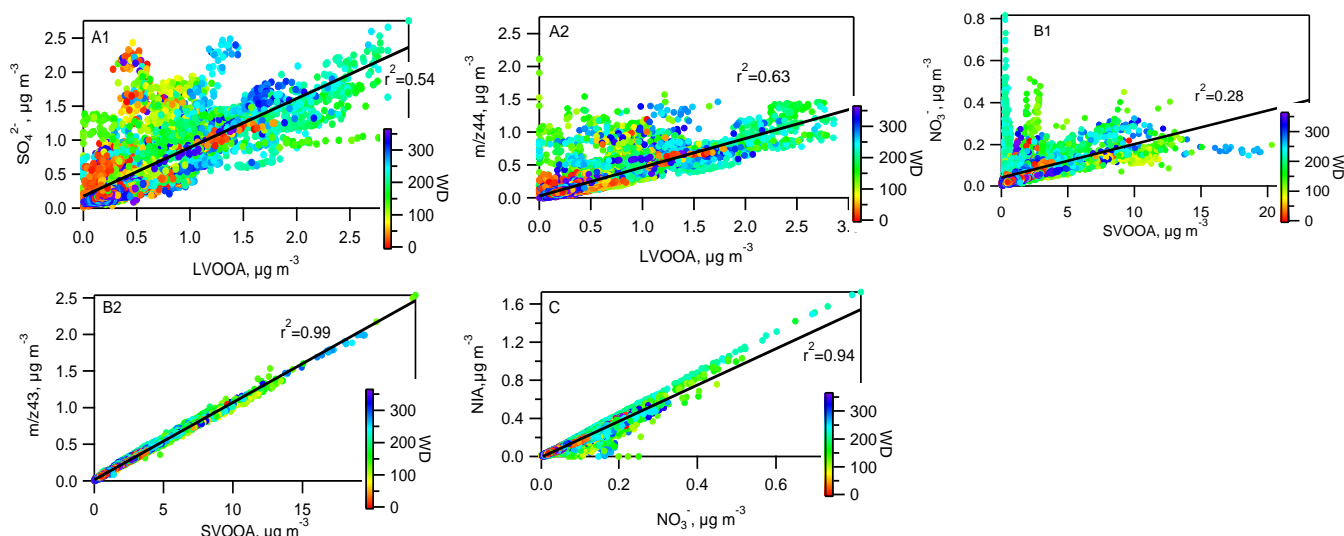

Figure S12. Correlation relationships of PMF factor with tracers. (a1) LVOOA vs. SO_4^{2-}; (a2)LVOOA vs. CO_2^+ ion; (b1) SVOOA vs NO_3^- ion; (b2) SVOOA vs m/z43 ion; (c)NIA vs NO_3^-.

The third factor, nitrate inorganic aerosol (NIA) factor, its mass spectrum is dominated by one prominent peak at m/z 30 (NO^+). The ratio of NO^+/NO_2^+ ions is 9.6 in this factor, which is greater than the value of 6.5 that was calibrated for the pure ammonium nitrate particles in this campaign. The NO^+/NO_2^+ ratios are usually in the range of 1.5 - 2.9 for pure NH_4NO_3 particles (Fry et al., 2009; Farmer et al., 2010). A higher ratio in this study is believed to be induced by the tuning of instrument (Farmer et al., 2010). The mass spectrum of NIA is similar to the NH_4NO_3 factor identified by PMF in several previous studies (Zhang et al., 2016; Kortelainen et al., 2017; Xu et al., 2015; Hao et al., 2014). However, the mass spectrum also contains organic signals such as CO_2^+ ions, suggesting that the factor is also interfered by organic fragments. The time series of the factor shows an excellent correlation with measured nitrate aerosol component ($r^2=0.94$). Thus, the factor is primarily recognized as a NH_4NO_3 factor.

Sec. S4. Evaluation of particulate organic nitrate by PMF

The estimation of amount of particulate organic nitrate aerosol followed the principles described in Hao et al., (2013, 2014). The methodology evaluates the organic nitrate concentration upon a sum of all the appointed NO^+ and NO_2^+ ions in the PMF organic factors. The principle hypothesizes that the distribution of NO_x ions between the organic and inorganic PMF factors corresponds to the separate existence of chemical forms of organic and inorganic nitrate (Hao et al.2014; Xu et al., 2015; Zhang et al., 2016). Thus, the mentioned above organic nitrates refer to the nitrate functional groups (-ONO_2). The terminology of organic nitrates is consistent with the ones in several studies (e.g. Kiendler-Scharr et al., 2016; Ng et al., 2016). A full calculation of organic nitrate molecules in terms of peroxy nitrates or alkyl nitrates (RO_2-NO_2 or RO-NO_2) needs to account for the corresponding organic fragments (R-, or RO-). In this study, the time series of organic nitrates and inorganic nitrates, diurnal cycles are shown in Fig. S13. The average mass concentration of organic nitrates was 0.01 $\pm$ 0.02 µg m^{-3} ($\pm$ s.d.), The organic nitrate aerosols play a role in the growth stage of newly formed particles and more discussion is provided in Sect. 3.4.
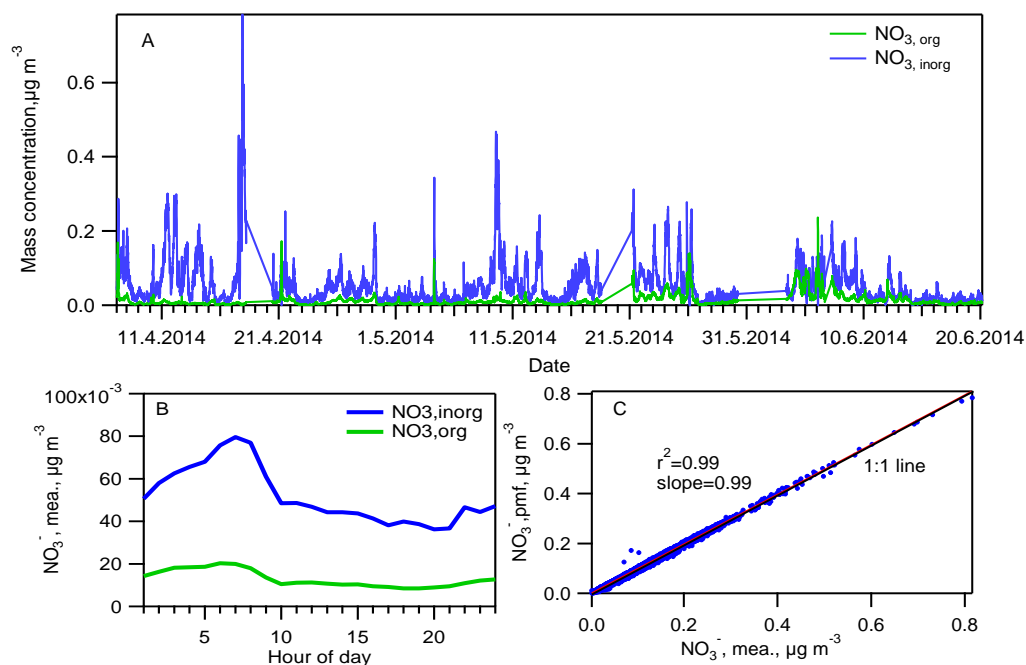
Figure S13. The separation of organic nitrates from inorganic nitrates by PMF in this study. (a): time series; (b): diurnal cycles; (c): comparison between the measured total nitrated to the simulated total nitrates by PMF.
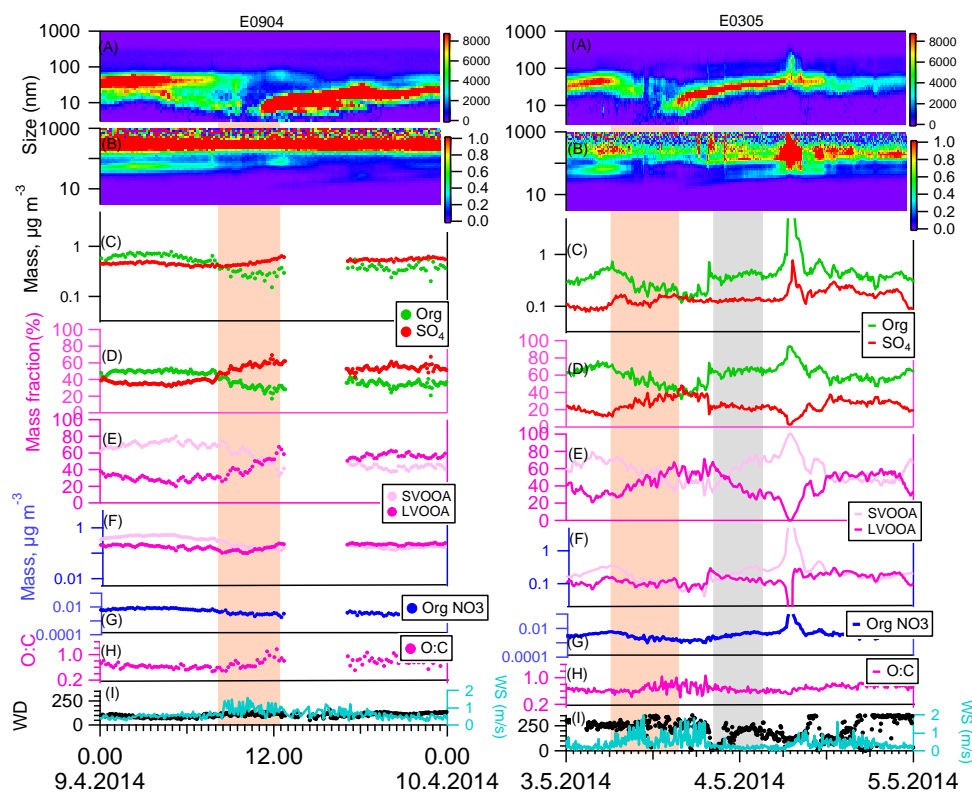
Figure S14. Observation of new particle formation events on 9 April 2014 (E0904) and 3 May 2014 (E0305). The orange bars were marked for the analysis before and right after nucleation and the gray bars were for aerosol growth periods. Panels: (a) aerosol number size distributions from DMPS; (b) volume size distributions from DMPS; (c) mass concentrations of organic (green) and sulfate (red) species by AMS; (d) mass fractions of organic and sulfate to total aerosol mass concentrations; (e) mass fractions of LVOOA (pink) and SVOOA (light pink) to total organic aerosol mass concentrations; (f) mass concentrations of LVOOA and SVOOA species determined by PMF; (g) the time series of organic nitrate aerosol; (h) O:C ratio of organic species by AMS; (i) wind speed (WS) and wind direction (WD). The data interruption in E0904 is due to measurement failure of AMS.

References

Allan, J. D., Alfarra, M. R., Bower, K. N., Coe, H., Jayne, J. T., Worsnop, D. R., Aalto, P. P., Kulmala, M., Hyötyläinen, T., Cavalli, F., and Laaksonen, A.: Size and composition measurements of background aerosol and new particle growth in a Finnish forest during QUEST 2 using an Aerodyne Aerosol Mass Spectrometer, Atmos. Chem. Phys., 6, 315-327, https://doi.org/10.5194/acp-6-315-2006, 2006.

Corrigan, A. L., Russell, L. M., Takahama, S., Äijälä, M., Ehn, M., Junninen, H., Rinne, J., Petäjä, T., Kulmala, M., Vogel, A. L., Hoffmann, T., Ebben, C. J., Geiger, F. M., Chhabra, P., Seinfeld, J. H., Worsnop, D. R., Song, W., Auld, J., and Williams, J.: Biogenic and biomass burning organic aerosol in a boreal forest at Hyytiälä, Finland, during HUMPPA-COPEC 2010, Atmos. Chem. Phys., 13, 12233-12256, https://doi.org/10.5194/acp-13-12233-2013, 2013.

Farmer, D. K., Matsunaga, A., Docherty, K. S., Surratt, J. D., Seinfeld, J. H., Ziemann, P. J., and Jimenez, J. L.: Response of an aerosol mass spectrometer to organonitrates and organosulfates and implications for atmospheric chemistry, Proc. Natl. Acad. Sci. U. S. A., 107, 6670–6675, https://doi.org/10.1073/pnas.0912340107, 2010.

Fry, J. L., Kiendler-Scharr, A., Rollins, A. W., Wooldridge, P. J., Brown, S. S., Fuchs, H., Dubé, W., Mensah, A., dal Maso, M., Tillmann, R., Dorn, H.-P., Brauers, T., and Cohen, R. C.: Organic nitrate and secondary organic aerosol yield from NO_3 oxidation of β-pinene evaluated using a gas-phase kinetics/aerosol partitioning model, Atmos. Chem. Phys., 9, 1431–1449, https://doi.org/10.5194/acp-9-1431-2009, 2009.

Ng, N. L., Brown, S. S., Archibald, A. T., Atlas, E., Cohen, R. C., Crowley, J. N., Day, D. A., Donahue, N. M., Fry, J. L., Fuchs, H., Griffin, R. J., Guzman, M. I., Herrmann, H., Hodzic, A., Iinuma, Y., Jimenez, J. L., Kiendler-Scharr, A., Lee, B. H., Luecken, D. J., Mao, J., McLaren, R., Mutzel, A., Osthoff, H. D., Ouyang, B., Picquet-Varrault, B., Platt, U., Pye, H. O. T., Rudich, Y., Schwantes, R. H., Shiraiwa, M., Stutz, J., Thornton, J. A., Tilgner, A., Williams, B. J., and Zaveri, R. A.: Nitrate radicals and biogenic volatile organic compounds: oxidation, mechanisms, and organic aerosol, Atmos. Chem. Phys., 17, 2103-2162, https://doi.org/10.5194/acp-17-2103-2017, 2017.

Ng, N. L., Canagaratna, M. R., Zhang, Q., Jimenez, J. L., Tian, J., Ulbrich, I. M., Kroll, J. H., Docherty, K. S., Chhabra, P. S., Bahreini, R., Murphy, S. M., Seinfeld, J. H., Hildebrandt, L., Donahue, N. M., DeCarlo, P. F., Lanz, V. A., Prévôt, A. S. H., Dinar, E., Rudich, Y., and Worsnop, D. R.: Organic aerosol components observed in Northern Hemispheric datasets from Aerosol Mass Spectrometry, Atmos. Chem. Phys., 10, 4625-4641, https://doi.org/10.5194/acp-10-4625-2010, 2010.

Hao, L. Q., Yli-Pirilä, P., Tiitta, P., Romakkaniemi, S., Vaattovaara, P., Kajos, M. K., Rinne, J., Heijari, J., Kortelainen, A., Miettinen, P., Kroll, J. H., Holopainen, J. K., Smith, J. N., Joutsensaari, J., Kulmala, M., Worsnop, D. R., and Laaksonen, A.: New particle formation from the oxidation of direct emissions of pine seedlings, Atmos. Chem. Phys., 9, 8121-8137, https://doi.org/10.5194/acp-9-8121-2009, 2009.

Hao, L. Q., Kortelainen, A., Romakkaniemi, S., Portin, H., Jaatinen, A., Leskinen, A., Komppula, M., Miettinen, P., Sueper, D., Pajunoja, A., Smith, J. N., Lehtinen, K. E. J., Worsnop, D. R., Laaksonen, A., and Virtanen, A.: Atmospheric submicron aerosol composition and particulate organic nitrate formation in a boreal forestland–urban mixed region, Atmos. Chem. Phys., 14, 13483-13495, https://doi.org/10.5194/acp-14-13483-2014, 2014.

Jordan, A., Haidacher, S., Hanel, G., Hartungen, E., Märk, L., Seehauser, H., Schottkowsky, R., Sulzer, P., and Märk, T. D.: A high resolution and high sensitivity proton-transfer-reaction time-of-flight mass spectrometer (PTR-TOF-MS), Int. J. Mass Spectrom., 286, 122–128, https://doi.org/10.1016/j.ijms.2009.07.005, 2009.

Kiendler-Scharr, A., Zhang, Q., Hohaus, T., Kleist, E., Mensan, A., Mentel, Th.F., Spindler, C., Uerlings, R., Tillmann, R., and Wildt, J.: Aerosol mass spectrometric features of biogenic SOA: Observations from a plant chamber and in rural atmospheric environments, Environ. Sci. Technol., 43, 8166-8172, https://doi.org/10.1021/es901420b, 2009.

Kiendler-Scharr, A., Mensah, A. A., Friese, E., Topping, D., Nemitz, E., Prevot, A. S. H., Äijälä, M., Allan, J., Canonaco, F., Canagaratna, M., Carbone, S., Crippa, M., Dall Osto, M., Day, D. A., De Carlo, P., Di Marco, C. F., Elbern, H., Eriksson, A., Freney, E., Hao, L., Herrmann, H., Hildebrandt, L., Hillamo, R., Jimenez, J. L., Laaksonen, A., McFiggans, G., Mohr, C., O'Dowd, C., Otjes, R., Ovadnevaite, J., Pandis, S. N., Poulain, L., Schlag, P., Sellegri, K., Swietlicki, E., Tiitta, P., Vermeulen, A., Wahner, A., Worsnop, D. and Wu, H., Ubiquity of organic nitrates from nighttime chemistry in the European submicron aerosol, Geophys. Res. Lett., 43, 7735-7744, https://doi.org/10.1002/2016GL069239, 2016.

Kortelainen, A., Hao, L., Tiitta, P., Jaatinen, A., Miettinen, P., Kulmala, M., Smith, J.N., Laaksonen, A., Worsnop, D.R., Virtanen,A., Sources of particulate organic nitrate in the boreal forest in Finland, Boreal Env. Res., 22, 13-26, www.borenv.net/BER/pdfs/ber22/ber22-013-026-Kortelainen.pdf, 2017.

Raatikainen, T., Vaattovaara, P., Tiitta, P., Miettinen, P., Rautiainen, J., Ehn, M., Kulmala, M., Laaksonen, A., and Worsnop, D. R.: Physicochemical properties and origin of organic groups detected in boreal forest using an aerosol mass spectrometer, Atmos. Chem. Phys., 10, 2063-2077, https://doi.org/10.5194/acp-10-2063-2010, 2010.

Rantala, P., Taipale, R., Aalto, J., Kajos, M. K., Patokoski, J., Ruuskanen, T. M. & Rinne, J.: Continuous flux measurements of VOCs using PTR-MS — reliability and feasibility of disjunct-eddy-covariance, surface-layer-gradient, and surface-layer-profile methods. Boreal Env. Res. 19 (suppl. B): 87–107, http://hdl.handle.net/10138/165182, 2014.

Schallhart, S., Rantala, P., Nemitz, E., Taipale, D., Tillmann, R., Mentel, T. F., Loubet, B., Gerosa, G., Finco, A., Rinne, J., and Ruuskanen, T. M.: Characterization of total ecosystem-scale biogenic VOC exchange at a Mediterranean oak–hornbeam forest, Atmos. Chem. Phys., 16, 7171-7194, https://doi.org/10.5194/acp-16-7171-2016, 2016.

Zhang, R.Y., Khalizov, A., Wang, L., Hu, M., Xu, W, Nucleation and growth of nanoparticles in the atmosphere, Chemical Reviews, 112, 1957-2011, https://doi.org/10.1021/cr2001756, 2012.

Xu, L., Suresh, S., Guo, H., Weber, R. J., and Ng, N. L.: Aerosol characterization over the southeastern United States using high-resolution aerosol mass spectrometry: spatial and seasonal variation of aerosol composition and sources with a focus on organic nitrates, Atmos. Chem. Phys., 15, 7307-7336, https://doi.org/10.5194/acp-15-7307-2015, 2015.